

Alma Mater Studiorum Università di Bologna  
Archivio istituzionale della ricerca

Novel dinuclear NHC–gold(i)-amido complexes and their application in energy transfer photocatalysis

This is the final peer-reviewed author's accepted manuscript (postprint) of the following publication:

*Published Version:*

Ma, X., Voloshkin, V.A., Martynova, E.A., Beliš, M., Peng, M., Villa, M., et al. (2023). Novel dinuclear NHC–gold(i)-amido complexes and their application in energy transfer photocatalysis. CATALYSIS SCIENCE & TECHNOLOGY, 13(14), 4168-4175 [10.1039/d3cy00716b].

*Availability:*

This version is available at: <https://hdl.handle.net/11585/962324> since: 2024-02-27

*Published:*

DOI: <http://doi.org/10.1039/d3cy00716b>









*Terms of use:*

Some rights reserved. The terms and conditions for the reuse of this version of the manuscript are specified in the publishing policy. For all terms of use and more information see the publisher's website.

This item was downloaded from IRIS Università di Bologna (<https://cris.unibo.it/>).  
When citing, please refer to the published version.

(Article begins on next page)

# Novel dinuclear NHC–gold(I)-amido complexes and their application in energy transfer photocatalysis†

Xinyuan Ma <sup>a</sup>, Vladislav A. Voloshkin <sup>‡</sup> <sup>a</sup>, Ekaterina A. Martynova <sup>‡</sup> <sup>a</sup>, Marek Beliš <sup>a</sup>, Min Peng <sup>a</sup>, Marco Villa <sup>b</sup>, Nikolaos V. Tzouras <sup>a</sup>, Wim Janssens <sup>a</sup>, Kristof Van Hecke <sup>a</sup>, Paola Ceroni <sup>b</sup> and Steven P. Nolan <sup>\*a</sup>

<sup>a</sup>Department of Chemistry and Centre for Sustainable Chemistry Ghent University, Krijgslaan 281, S-3, 9000 Ghent, Belgium. E-mail: [steven.nolan@ugent.be](mailto:steven.nolan@ugent.be); Web: <https://www.nolan.ugent.be>

<sup>b</sup>Department of Chemistry “Giacomo Ciamician”, University of Bologna, Via Selmi, 2, 40126 Bologna, Italy

## Abstract

The development of efficient and operationally simple synthetic routes to dinuclear gold(I)-amido complexes bearing aromatic/aliphatic-bridges are reported. This family of complexes was prepared utilizing environmentally friendly and sustainable reagents under mild conditions, resulting in 68–92% yields of the targeted compounds. These novel dinuclear gold(I)-amido complexes were structurally and spectroscopically characterized. Their photophysical properties were also studied. This series of gold complexes are phosphorescent with lifetimes in the hundreds of microseconds range. They exhibit high catalytic activity as photosensitizers in intramolecular cycloaddition and cyclization reactions at catalyst loadings ranging from 0.5 to 2 mol%.

---

## Introduction

Photoactive transition metal complexes are widely used in photocatalysis, organic electronics, and dye-sensitized solar cells due to their tuneable photophysical properties.<sup>1</sup> In particular, luminescent materials with efficient microsecond phosphorescence have emerged as highly promising candidates for application in organic light-emitting diodes (OLEDs).<sup>2</sup> During the last five years, several reports of highly luminescent, two-coordinate, d<sup>10</sup> metal complexes of coinage metals (*i.e.*, Cu, Ag, Au) have appeared.<sup>3</sup> Carbene–metal–amido (CMA) complexes containing *N*-heterocyclic carbene (NHC) ligands have drawn particular attention in these luminescence related areas.<sup>4</sup> From a structural point of view, these tuneable emitters with donor–bridge–

acceptor designs are composed of amido fragments usually based on the carbazole template, acting as donor and carbene-type acceptor ligands.<sup>5</sup> Unlike some of the early reported Ir- and Ru-based emitters,<sup>6</sup> these coinage-metal-based complexes emit predominantly *via* thermally assisted delayed fluorescence (TADF), while the former rely on strong spin-orbit coupling to induce emission.<sup>2,7</sup> The TADF emission in these CMA complexes predominantly originates from ligand to ligand charge transfer (LLCT) states. Currently, some of the carbazolyl-bearing CMA emitters with M = Cu, Ag, Au have found applications in OLED devices and as photocatalysis by selecting an appropriate carbene as ligand.<sup>4a-c,5</sup>

To our knowledge, the carbazolyl-based CMAs have been reported mainly bearing cyclic alkylaminocarbene (CAAC),<sup>4a,b,d,8</sup> mono- or diamidocarbene (MAC or DAC),<sup>2,4c</sup> as well as imidazol(in)-ylidene ligands<sup>5b,9</sup> and 1,3-thiazoline carbene<sup>10</sup> (Fig. 1). The vast majority of amido-bearing complexes are usually synthesized from [M(NHC)Cl] complexes (M = Cu, Ag, Au) as starting material in conjunction with strong bases, such as KO<sup>t</sup>Bu, NaO<sup>t</sup>Bu, or KHMDS, to achieve carbazole N-H metallation.<sup>4b,c,5b,8</sup> In addition, the formation of [M(NHC)(amido)] complexes can also be achieved by pre-activation of amides or by ligand exchange.<sup>10</sup> The reported synthetic routes usually require strictly inert conditions, cumbersome workup, needed subsequent purification steps and long reaction times.

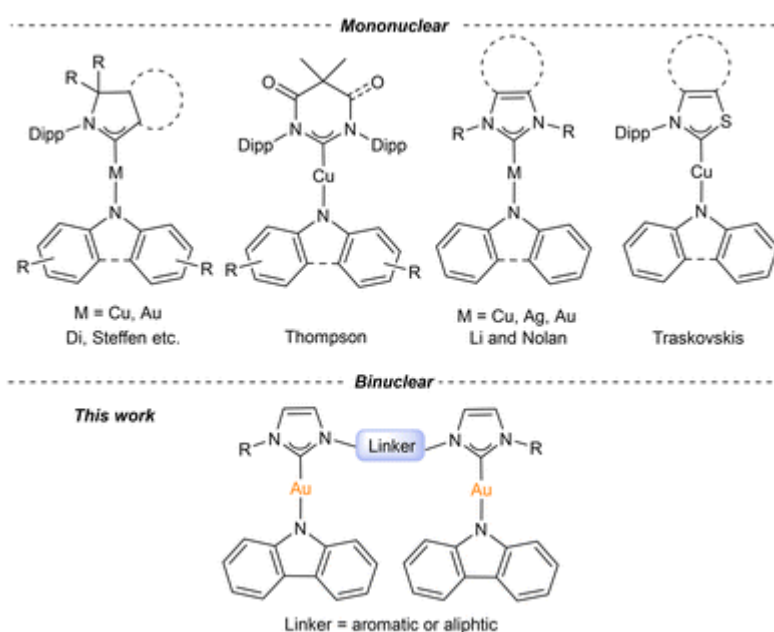


**Fig. 1** Carbene–metal–amido (CMA) emitters/sensitizers.

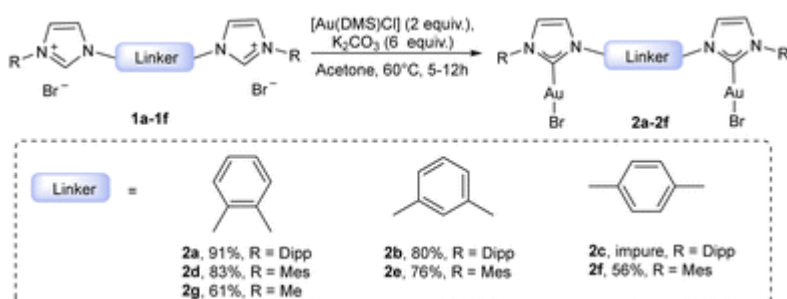
Recently, we have reported a simple and efficient route to various [M(NHC)(amido)] complexes (M = Cu, Ag and Au) involving the use of a weak base and environmentally friendly solvents under mild conditions.<sup>5c,9b,c</sup> These compounds have been successfully applied in organic synthesis<sup>9c</sup> and photocatalysis.<sup>11</sup> In addition, some of the CMA complexes have shown remarkable anticancer activity in several cell lines.<sup>9b,d</sup> To the best of our knowledge, all reported CMA complexes are

mononuclear and dinuclear amido-bearing NHC complexes have not yet been described in the literature.

Dinuclear gold(I) complexes have been known since the 1970s and have attracted significant attention since.<sup>12</sup> A series of digold(I) species has been isolated and these have provided important insights into dual activation reaction mechanisms.<sup>13</sup> In addition, several more recently synthesized dinuclear gold(I) complexes have been extensively studied in catalysis,<sup>14</sup> materials science<sup>15</sup> and as promising anticancer agents.<sup>16</sup> Nevertheless, they have been significantly less studied than their mononuclear counterparts. Therefore, the design of new digold(I) complexes is still needed and can possibly further probe the fundamental question of synergistic bimetallic interactions and their influence on catalytic behaviour and reactivity.

Intrigued by various applications of mononuclear NHC–gold–amido complexes in photocatalysis, medicinal chemistry and as photo-emissive materials,<sup>3,4a-c,5</sup> and given the lack of current reports regarding dinuclear metal complexes with bridging NHC linkers, we now report on this class of dinuclear NHC–gold(I)–amido complexes.

Initially, our investigation dealt with the synthesis of dinuclear bridged NHC–Au–Br precursors ([Scheme 1](#)). Based on our previous experience and literature reports,<sup>17</sup> a family of aryl-bridging complexes  $[(L)Au_2Br_2]$  (L = bridged bis(NHC)) **2a–b** and **2d–f** was successfully synthesized in good to excellent yields from the corresponding bisNHC salts with  $[Au(DMS)Cl]$  in the presence of weak base, namely  $K_2CO_3$  at 60 °C in acetone under aerobic conditions. Unexpectedly, the *p*-xylene as a linker results in rapid decomposition of the gold compound. Therefore, the bis(IMes) complex **2f** was isolated in only moderate yield. Unfortunately, pure **2c** could not be obtained even after several attempts. Reasons for this are unknown at this time.

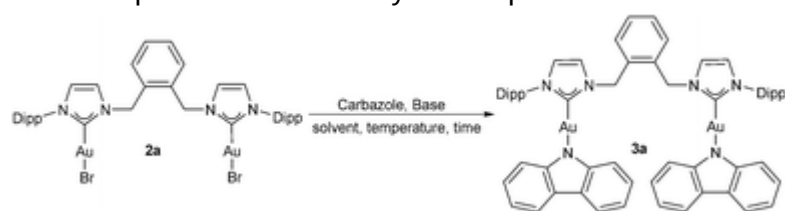


**Scheme 1** The scope of various dinuclear bridging NHC–Au–Br complexes.

With the  $[(L)Au_2Br_2]$  precursors in hand, we moved to the synthesis of digold-containing NHC carbazolyl complexes. We began optimization of the reaction conditions with the model reaction of  $[(IPr)^{o\text{-xylene}}(AuBr)_2]$  **2a** with 2.2 equiv. of carbazole and 6 equiv. of  $K_2CO_3$  in acetone at 60 °C ([Table](#)

1, entry 1). Gratifyingly, the desired complex  $[(\text{IPr})^{o\text{-xylene}}(\text{AuCbz})_2]$  (Cbz = carbazole) **3a** was obtained after 6 hours in an 83% yield. The use of EtOH as a solvent led to the slight decrease in yield to 79% (Table 1, entry 2). In the case of EtOAc as a solvent, no product was observed, even after prolonged reaction times (Table 1, entry 3). Decreasing the temperature led to longer reaction times to achieve full conversion and resulted in a 71% isolated yield. Next, the influence of the amount of base used was investigated. Identical yields were obtained when 4 equiv. instead of 6 equiv. were used. Finally, the same isolated yield as in entry 1 was obtained by further reducing the reagent amount to 2 equiv. of carbazole with 4 equiv. of  $\text{K}_2\text{CO}_3$  and a reaction time of 10 hours. We also examined the efficiency of other weak bases such as  $\text{NEt}_3$  and  $\text{NaOAc}$ , which confirmed potassium carbonate as the optimal base for this reaction (Table 1, entries 7–8). We reasoned that  $\text{NaOAc}$  ( $\text{p}K_a = 4.7$ ) is not sufficiently basic to achieve N–H metallation. Results with the use of  $\text{NEt}_3$  as a base agree with those found for the synthesis of mononuclear carbazolyl complexes.<sup>5c</sup>

**Table 1** Optimization of the synthetic protocol<sup>a</sup>



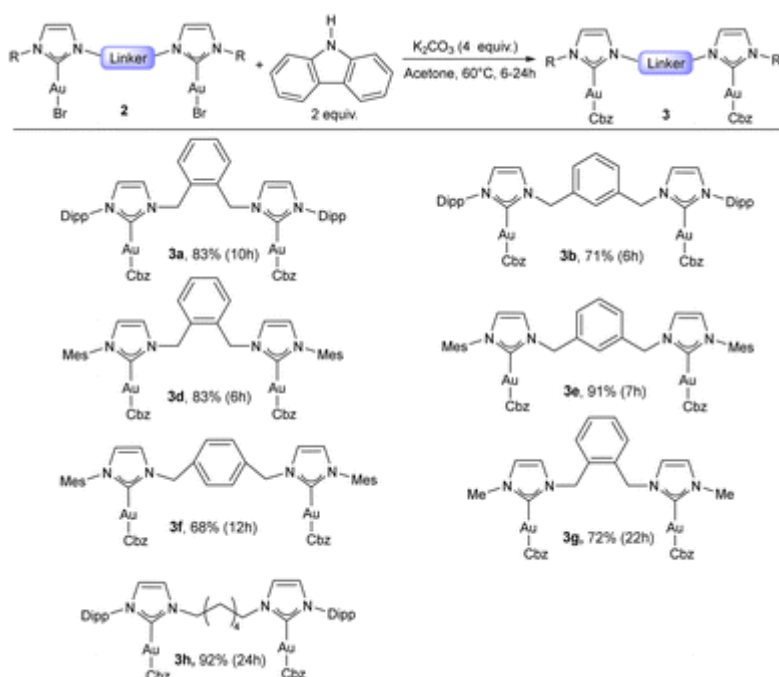
Entry	Base (equiv.)	Solvent	Temp. (°C)	Time (h)	Yield <sup>b</sup> (%)
-------	---------------	---------	------------	----------	------------------------

<sup>a</sup> Reaction conditions:  $[\text{Au}(\text{NHC})\text{Br}]_2$  (0.1 mmol, 1 equiv., 111.2 mg), carbazole (2.2 equiv., 36.8 mg),  $\text{K}_2\text{CO}_3$  (6 equiv., 82.9 mg) in 1 mL of acetone at 60 °C. <sup>b</sup> Isolated yields. <sup>c</sup> 4 equiv. of base. <sup>d</sup> 2 equiv. of carbazole.

1	$\text{K}_2\text{CO}_3$	Acetone	60	6	83
2	$\text{K}_2\text{CO}_3$	EtOH	40	6	79
3	$\text{K}_2\text{CO}_3$	EtOAc	40	12	Trace
4	$\text{K}_2\text{CO}_3$	Acetone	rt	12	71
5 <sup>c</sup>	$\text{K}_2\text{CO}_3$	Acetone	60	10	81
<b>6</b>	<b><math>\text{K}_2\text{CO}_3</math></b>	<b>Acetone</b>	<b>60</b>	<b>10</b>	<b>83</b>
7 <sup>c</sup>	$\text{NaOAc}$	Acetone	60	12	Trace
8 <sup>c</sup>	$\text{Et}_3\text{N}$	Acetone	60	12	Trace

With the optimized reaction conditions in hand, carbazolyl dinuclear NHC complexes **3a–3h** were synthesized from the corresponding  $[(\text{L})(\text{AuBr})_2]$  precursors and carbazole in the presence of  $\text{K}_2\text{CO}_3$  in acetone. A series of bis(NHC)-bearing carbazolyl complexes as off-white solid were obtained in moderate to excellent yields (Scheme 2). To our delight, the weak base route

proves to be highly efficient for most all of the bis(NHC) complexes examined, **2a–b** and **2d–2h**. Moreover, the method can be successfully applied not only to the bis(NHC)-bearing carbazolyl complexes bearing aromatic linkers, but also to dinuclear gold–carbazolyl complex bearing an aliphatic linker ([Scheme 2](#), **3h**). Notably, in the case of NHC with *p*-aryl linker, isolated yields were lower compared to the ones bearing *o*- or *m*-aryl linkers ([Scheme 2](#), **3d** and **3e**vs.**3f**). Despite sterically smaller NHC ligand, a longer reaction time was needed to obtain bis[NHC–Au–carbazolyl] complex **3g** from the **2g** precursor.



**Scheme 2** Synthetic reaction scope for dinuclear bridging NHC–Au–Cbz complexes.

To confirm the structure of members of this new family of complexes, all of them were characterized by  $^1H$  and  $^{13}C$  NMR spectroscopy. All complexes were stable under air and even in solution (such as DMSO, DCM or MeOH) for several days. It is worth mentioning that some of them, namely, **3b**, **3e**, **3f** and **3g** are poorly soluble in  $CDCl_3$ , acetone- $d_6$  or  $CD_2Cl_2$ , and that DMSO- $d_6$  was usually employed as the NMR solvent to achieve the spectroscopic analysis. In addition, crystals suitable for single crystal XRD analysis were grown for complexes **3e** and **3c** ([Fig. 2](#)). The structures of both complexes reveal no intramolecular interactions between gold atoms. The distance between the two gold centers in **3c** with *p*-aryl linker (9.0390(5) Å) is significantly longer than the distance found in **3e** bearing a *m*-aryl linker (6.273(1) Å). The X-ray structures of **3c** and **3e** show that the plane of the carbazolyl fragment adopts a vertical orientation with respect to the plane of the aryl linker. It is worth noting that both carbazolyl and imidazolylidene moieties of

structure **3e** are almost parallel to each other. The cause of this structural arrangement is the mandated orientation of the two gold centers *via* the linker substitution pattern. However, these two fragments extend away from the *m*-xylene core. The detailed structural data can be found in the ESI† in Tables S3 and S4.

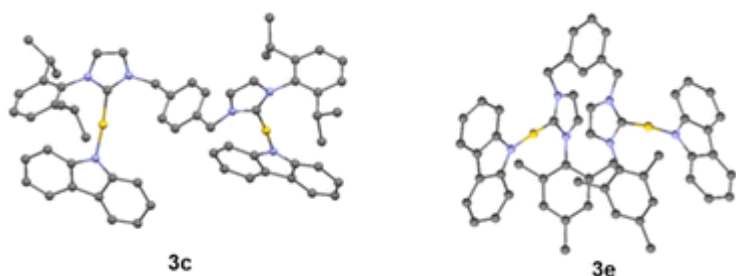
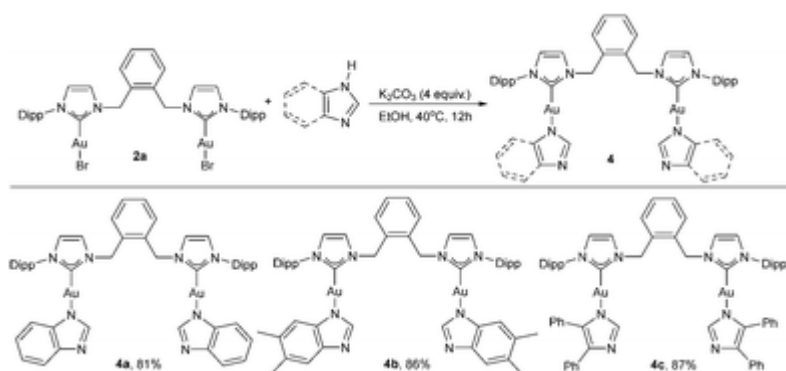


**Fig. 2** X-ray molecular structures of **3c** and **3e**, showing thermal displacement ellipsoids at the 50% probability level (omitted for clarity (see ESI† for more detailed structural information). CCDC [2213682](#) and [2213683](#) (**3c** and **3e**)).

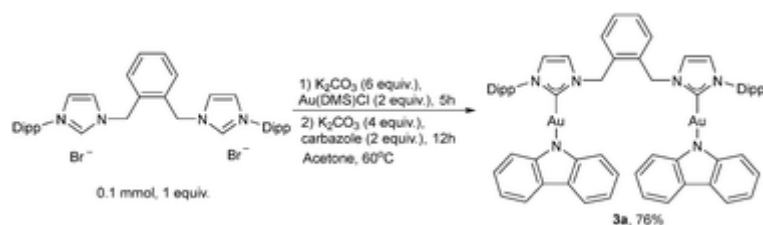
Considering the increasing interest of the application of gold complexes in medicinal chemistry and the recently reported promising antitumor activity of mononuclear CMA complexes *in vitro*,<sup>9d</sup> we turned our attention to the synthesis of bisNHC gold-amido complexes bearing other *N*-heterocycles ([Scheme 3](#)).



**Scheme 3** The scope of NHC–Au–amido complexes.

We noticed that when EtOH was used as the solvent, the obtained yields proved slightly higher than in acetone. Therefore, a series of  $[(L)\{Au(amido)\}_2]$  (**4a–4c**) complexes were synthesized in excellent yields by employing various amines with higher acidity than carbazole in EtOH as a solvent and  $K_2CO_3$  as base. It is worth mentioning that no conversion was observed with 10*H*-phenothiazine ( $pK_a = 23$ ), we assume the reason for this is its lower acidity compared with carbazole ( $pK_a = 19.9$ ), benzimidazole ( $pK_a = 12.8$ ), 5,6-dimethylbenzimidazole ( $pK_a = 13.5$ ) or 4,5-diphenylimidazole ( $pK_a = 13$ ). Unexpectedly, the reaction involving diphenylamine ( $pK_a = 0.79$ ) yielded an impure NHC–Au–amido complex.

To test the compatibility of the metalation involving the imidazolium salt and the carbazole metalation steps, a one-pot synthesis of dinuclear NHC–Au–Cbz compound was successfully performed directly from the imidazolium salt and the metal source, and the desired [(IPr)<sup>o</sup>-xylene{Au(Cbz)}<sub>2</sub>] **3a** was obtained in high purity and yield ([Scheme 4](#)).



**Scheme 4** One-pot synthesis of dinuclear CMA complex.

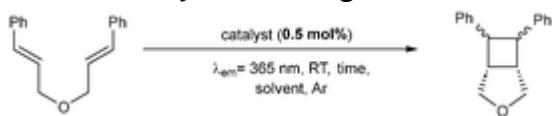
Having recently reported on the use of [Au(SIPr)(Cbz)](**PhotAucat 1**) and [Au(IPr)(Cbz)](**PhotAucat 2**) as sensitizers in the [2 + 2] cycloaddition of diallyl ethers and *N*-tosylamides and having also shown that these gold–NHC complexes enabled the unprecedented photocatalytic intramolecular [2 + 2] cycloaddition of indoles,<sup>5c,11</sup> the structural similarities between these photocatalysts and the novel dinuclear [(bisNHC){Au(Cbz)}<sub>2</sub>] complexes described here, we reasoned that two gold centers might also prove beneficial in EnT photocatalysis.<sup>18,19</sup> We next investigated the photocatalytic activity and photophysical properties of the new family of dinuclear bridging complexes to validate these suspicions.

We began our investigation into the [2 + 2] cycloaddition by selecting the model reaction targeting the intramolecular reaction of ((1*E*,1'*E*)-oxybis(prop-1-ene-3,1-diyl))dibenzene ([Table 2](#)). In order to compare all dinuclear catalysts with the state-of-the-art [Au(SIPr)(Cbz)], the photocatalytic reactions were conducted in THF, due to the higher solubility of some of the catalysts ([Table 2](#)). As a benchmark, we used the previously reported results where the **PhotAucat 1** sensitizer provided an 80% conversion with 1 mol% catalyst loading after 30 min. To keep the same [Au–Cbz] loading, 0.5 mol% of dinuclear complexes were used in this screening. Surprisingly, an excellent conversion of >90% was observed with most tested carbazole-based catalysts **3**, but not with **3h**. Most complexes showed superior performance when compared with **PhotAucat 1**. With these exciting results in hand, the reaction time was decreased to 15 min to identify the best catalyst. The highest conversion (84%) was achieved when **3a** was used as sensitizer ([Table 2](#), entry 1), an 80% conversion was observed for the **3b** and **3e** congeners ([Table 2](#), entries 4, 8). Other dinuclear gold–NHC complexes, bearing various amido moieties were inefficient in this model reaction ([Table 2](#), entries 15–17). In order to confirm that the dinuclear



bridging [bis(NHC){Au(Cbz)}<sub>2</sub>] complexes could be compatible with greener reaction conditions, a reaction in EtOAc as solvent was performed and it proved as efficient as when it was performed in THF (Table 2, entry 2). Control experiments confirmed the need for both sensitizer and light for the reaction to proceed (Table 2, entries 20 and 21).

**Table 2** Catalyst screening for the [2 + 2] cycloaddition of diallyl ether



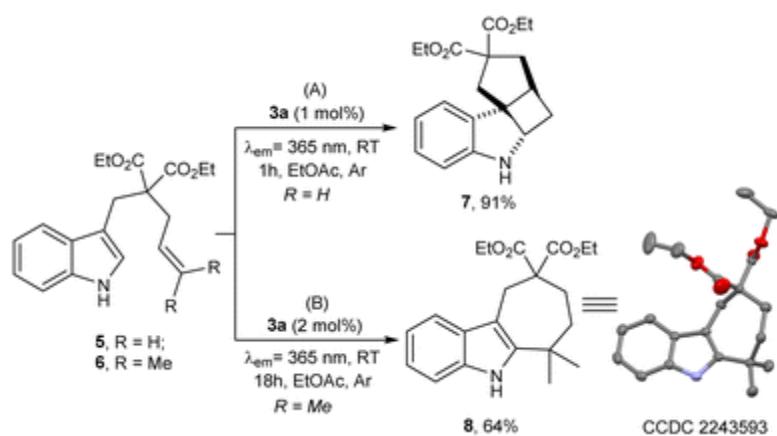
Entry	Catalyst	Solvent	Time, GC	
			min	conversion <sup>a</sup> (%)

<sup>a</sup> Conversion was determined by GC using dodecane as internal standard and is the average of 2 reactions. <sup>b</sup> The data were taken from our previous report.<sup>11</sup>

1	<b>3a</b>	THF	15	84
2		EtOAc	15	86
3		THF	30	97
4	<b>3b</b>	THF	15	80
5			30	94
6	<b>3d</b>	THF	15	77
7			30	97
8	<b>3e</b>	THF	15	80
9			30	98
10	<b>3f</b>	THF	15	60
11			30	90
12	<b>3g</b>	THF	15	73
13			30	92
14	<b>3h</b>	THF	30	84
15	<b>4a</b>	THF	15	<10
16	<b>4b</b>	THF	15	<10
17	<b>4c</b>	THF	15	<10
18 <sup>b</sup>	[Au(SIPr)(Cbz)]	THF	15	76
19 <sup>b</sup>	(1 mol%)		30	80
20	Without <b>3a</b>	THF	60	<10
21	<b>3a</b> (in the dark)	THF	30	<10

To demonstrate the effectiveness of the dinuclear gold sensitizers in challenging photocatalytic reactions, the [2 + 2] cycloaddition of an unprotected indole which proved impossible with organo- or iridium-based sensitizers,<sup>20</sup> was tested.<sup>11</sup> Gratifyingly, complete conversion of diethyl 2-((1*H*-indol-3-yl)methyl)-2-allylmalonate **5** was achieved after 1 h in the

presence of 1 mol% of **3a**, **3b**, **3d** or **3e** (Scheme 5, A; ESI,† Table S1). Complex **3f** exhibited low catalytic efficiency for the cycloaddition of indole with only a 50% conversion, due most likely to the poor solubility of this complex in EtOAc. Using sensitizer **3a**, the desired cycloaddition product **7** was isolated in 91% yield, a catalytic performance equivalent to that of mononuclear gold complexes.<sup>11</sup> The success of this reaction shows how the range of substrates can be extended beyond that permitted with reported organo- or Ir-based sensitizers *via* energy transfer photocatalysis.



**Scheme 5** Energy transfer catalysis of unprotected indoles.

Inspired by this result, we turned our interest to cyclization of dimethyl-substituted indole **6** (Scheme 5, B; and ESI,† Table S2). However, no sign of the desired product was observed after 1 h of irradiation, even with a catalyst loading of 2 mol%. Interestingly, we observed some conversion of starting material and therefore prolonged the reaction time. After 18 hours of irradiation, a 74% conversion of indole **6** was reached. Only one major product was detected in the NMR spectrum of the reaction crude; however, the generated compound did not prove to be the expected cyclobutane-containing product.

Surprisingly, the isolated product was identified as cyclohepta[*b*]indole **8** by NMR analysis. Furthermore, its structure was confirmed with HRMS and diffraction study of single crystal (Scheme 5, B). The presence of two methyl groups on the double bond of **6** impedes the [2 + 2] cycloaddition and leads instead to a cyclization product **8**. It should be noted that such cyclohepta[*b*]indole motifs are present in a wide range of natural products and biologically active molecules and is of significant relevance in drug design.<sup>21</sup> Further study of this photochemical transformation is underway in our laboratory to explore the generality of the transformation and results will be presented in due course.

In order to compare the photophysical properties of the new dinuclear complexes with those of the previously reported  $[\text{Au}(\text{IPr})(\text{Cbz})]$ , we recorded their absorption, excitation and emission spectra in THF or DMSO solutions and only insignificant differences were observed for these two solvents. All obtained spectra for each compound are presented in the ESI.†

The absorption spectra of all carbazole-containing complexes are very similar to each other and to the previously reported absorption spectrum of **PhotAucat 1** (Fig. 3). They consist of similarly overlapped bands and shoulders in the range of 250–385 nm. The maxima at *ca.* 275 nm and 310 nm were previously assigned to ligand-centered (LC) transitions of carbazole and NHC ligands. The broad band with a shoulder at 315–360 nm is almost identical for all complexes with the only exception of **3h** due to less extended aromaticity. This band is slightly shifted hypsochromically. It is worth noting, that this is the only complex with an alkyl linker, which apparently effects the shape of this band, previously assigned to ligand-to-ligand charge transfer (LLCT) from Cbz to NHC. The weak band at *ca.* 370 nm is independent of the linker or NHC ligand used, which is in accordance with symmetry forbidden MLCT transition Au–Cbz. The molar absorption coefficients ( $\epsilon$ ) for **3g** was not determined due to its low solubility.

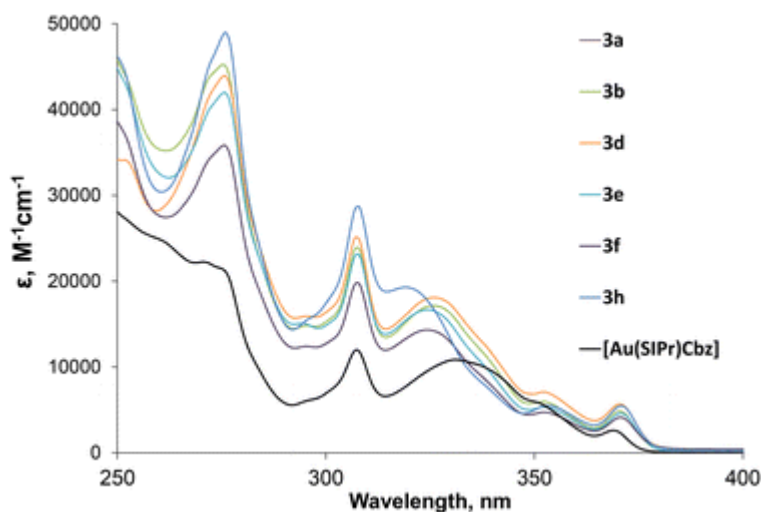


**Fig. 3** Absorption spectra of complexes **3** in solution.

Interestingly,  $\epsilon$  of **3a–b**, **3d–3f** and **3h** are *ca.* 2-fold higher than the one found for **PhotAucat 1**. This result is in accordance with the two NHC–Au–Cbz moieties of the complexes acting independently of each other without any interaction. Emission spectra of all complexes also support this hypothesis, being almost identical to the **PhotAucat 1** sensitizer without any additional noticeable features (Fig. 4). All gold complexes are phosphorescent with lifetimes in the microseconds range. Substitution of imidazolylidene with aromatic groups (**3a–f**) significantly

increases the lifetimes ( $\tau = 126\text{--}262 \mu\text{s}$ ) and also the emission quantum yields ( $\Phi = 37\text{--}77\%$ ) compared to aliphatic substitution (**3g**,  $\tau = 48 \mu\text{s}$ ,  $\Phi = 16\%$ ) (see ESI,† Table S3). The emission maxima for all complexes are at 430–431 nm, except for **3g**, which emits at 434 nm, a minor difference. Therefore, no significant effect is observed on the energy of the lower excited state was observed by varying the imidazolylidene substitution or by changing the insulating linker. These values correspond to  $E_T$  values of 65.9 kcal mol<sup>-1</sup> for **3g** and 66.3–66.5 kcal mol<sup>-1</sup> for the other complexes. This difference could potentially explain why **3g** performed slightly less efficiently than its congeners. As triplet energy values of the complexes are close to the one of **PhotAucat 1**, they are expected to perform similarly in the same [2 + 2] cycloaddition reaction. However, the reasons for the slightly higher conversion rates observed for the dinuclear complexes are unclear at this time and are presently being investigated.

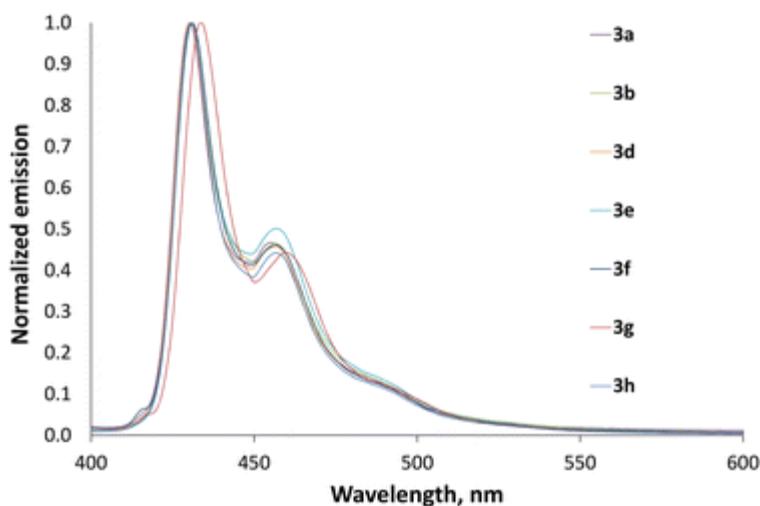


**Fig. 4** Emission spectra of complexes **3**.

The experimental data clearly indicate that the new dinuclear complexes can be utilized in energy transfer photocatalysis as were the previously reported **PhotAucat 1** and **PhotAucat 2** complexes. The new dinuclear complexes prove as or slightly more efficient than their mononuclear cousins.

## Conclusions

A series of dinuclear CMA complexes bearing aromatic/aliphatic linkers has been prepared for the first time. This new class of dinuclear NHC–gold-amido complexes bearing aromatic or aliphatic linker has been synthesized *via* efficient and operationally simple synthetic routes under mild conditions. This straightforward synthetic protocol shows broad compatibility with NHC ligands bearing different substituents and linkers. The novel CMAs were structurally characterized, and representative complexes were analyzed by single crystal diffraction. Dinuclear gold–Cbz complexes were tested as sensitizers in the [2 + 2] intramolecular addition of dicinnamyl ether

and indole **6**, exhibiting excellent catalytic activity. The observed reaction profiling using the dinuclear species as sensitizers showed that conversion could be achieved in shorter times than when the mononuclear [Au(SIPr)(Cbz)] complex was used. In addition, an unexpected cyclohepta[*b*]indole product **8** was obtained when the indole substrate was decorated with two methyl substituents. This series of gold complexes exhibits an emission in the 430–434 nm range with long lifetimes (hundreds of microseconds). Overall, the photophysical properties of the dinuclear complexes are reminiscent to the ones for [Au(SIPr)(Cbz)], indicating that two NHC–Au–Cbz fragments of the molecule are independent in solution and do not display any cooperative interaction. Further studies are presently being performed in our laboratory to shed light on the slightly higher efficiency of these dinuclear complexes. These are also being deployed in related photocatalytic reactions.

## Conflicts of interest

There are no conflicts to declare.

## Acknowledgements

We gratefully acknowledge VLAIO (SBO project CO2PERATE). The Special Research Fund (BOF) of Ghent University is also acknowledged (starting and senior grants to SPN). XM and MP thank the China Scholarship Council (CSC) (project 201908530217 and 201806910084) for PhD fellowships. KVH and MB (project G099319N) and SPN (project G0A6823N) thank the Research Foundation – Flanders (FWO) for financial support. P. C. and M. V. acknowledge the University of Bologna for support.

## Notes and references

1. (a) E. M. Poland and C. C. Ho, *Appl. Organomet. Chem.*, 2022, e6746 [Search PubMed](#); (b) K. Li, Y. Chen, J. Wang and C. Yang, *Coord. Chem. Rev.*, 2021, **433**, 213755–213770 [CrossRef](#) [CAS](#); (c) M. H. Keefe, K. D. Benkstein and J. T. Hupp, *Coord. Chem. Rev.*, 2000, **205**, 201–228 [CrossRef](#) [CAS](#); (d) M. Grätzel, *Inorg. Chem.*, 2005, **44**, 6841–6851 [CrossRef](#).
2. R. Hamze, S. Shi, S. C. Kapper, D. S. M. Ravinson, L. Estergreen, M.-C. Jung, A. C. Tadler, R. Haiges, P. I. Djurovich, J. L. Peltier, R. Jazzar, G. Bertrand, S. E. Bradforth and M. E. Thompson, *J. Am. Chem. Soc.*, 2019, **141**, 8616–8626 [CrossRef](#) [CAS](#) [PubMed](#).
3. (a) F.-H. Yu, X.-F. Song, G.-H. Liu, X. Chang, K. Li, Y. Wang, G. Cui and Y. Chen, *Chem. – Eur. J.*, 2022, e20220243 [Search PubMed](#); (b) R. Hamze, M. Idris, D. S. M. Ravinson, M. C. Jung, R. Haiges, P. I. Djurovich and M. E. Thompson, *Front. Chem.*, 2020, **8**, 401–409 [CrossRef](#) [CAS](#) [PubMed](#); (c) S. Cai, G. S. M. Tong, L. Du, G. Kwok-Ming So, F.-F. Hung, T.-L. Lam, G. Cheng, H. Xiao, X. Chang, Z.-X. Xu and C.-M. Che, *Angew. Chem.*, 2022, **61**, e202213392 [CAS](#); (d) R. Tang, S. Xu, T.-L. Lam, G. Cheng, L. Du, Q. Wan, J. Yang, F.-F. Hung, K.-H. Low, D. L. Phillips and C. M. Che, *Angew. Chem.*, 2022, **61**, e202203982 [CAS](#); (e) J.-G. Yang, X.-F. Song, J. Wang, K. Li, X. Chang, L.-Y. Tan, C.-X. Liu, F.-H. Yu, G. Cui, G. Cheng, W.-P. To, C. Yang, C.-M. Che and Y. Chen, *Chem. – Eur. J.*, 2021, **27**, 17834–

- 17842 [CrossRef](#) [CAS](#) [PubMed](#) ; (f) L. K. Li, C. C. Au-Yeung, M. C. Tang, S. L. Lai, W. L. Cheung, M. Ng, M. Y. Chan and V. W. W. Yam, *Mater. Horiz.*, 2022, **9**, 281–293 [RSC](#) ; (g) W. K. Kwok, M. C. Tang, S. L. Lai, W. L. Cheung, L. K. Li, M. Ng, M. Y. Chan and V. W. W. Yam, *Angew. Chem., Int. Ed.*, 2020, **59**, 9684–9692 [CrossRef](#) [CAS](#) [PubMed](#) .
4. (a) D. Di, A. S. Romanov, L. Yang, J. M. Richter, J. P. H. Rivett, S. Jones, T. H. Thomas, M. Abdi Jalebi, R. H. Friend, M. Linnolahti, M. Bochmann and D. Credgington, *Science*, 2017, **356**, 159–163 [CrossRef](#) [CAS](#) [PubMed](#) ; (b) R. Hamze, J. L. Peltier, D. Sylvinson, M. Jung, J. Cardenas, R. Haiges, M. Soleilhavoup, R. Jazzar, P. I. Djurovich, G. Bertrand and M. E. Thompson, *Science*, 2019, **363**, 601–606 [CrossRef](#) [CAS](#) [PubMed](#) ; (c) S. Shi, M. C. Jung, C. Coburn, A. Tadde, D. M. R. Sylvinson, P. I. Djurovich, S. R. Forrest and M. E. Thompson, *J. Am. Chem. Soc.*, 2019, **141**, 3576–3588 [CrossRef](#) [CAS](#) [PubMed](#) ; (d) A. S. Romanov, S. T. E. Jones, L. Yang, P. J. Conaghan, D. Di, M. Linnolahti, D. Credgington and M. Bochmann, *Adv. Opt. Mater.*, 2018, **6**, 1801347 [CrossRef](#) ; (e) A. S. Romanov, C. R. Becker, C. E. James, D. Di, D. Credgington, M. Linnolahti and M. Bochmann, *Chem. – Eur. J.*, 2017, **23**, 4625–4637 [CrossRef](#) [CAS](#) [PubMed](#) .
5. (a) J. Föllner and C. M. Marian, *J. Phys. Chem. Lett.*, 2017, **8**, 5643–5647 [CrossRef](#) [PubMed](#) ; (b) A. S. Romanov, L. Yang, S. T. E. Jones, D. Di, O. J. Morley, B. H. Drummond, A. P. M. Reponen, M. Linnolahti, D. Credgington and M. Bochmann, *Chem. Mater.*, 2019, **31**, 3613–3623 [CrossRef](#) [CAS](#) ; (c) N. V. Tzouras, E. A. Martynova, X. Ma, T. Scattolin, B. Hupp, H. Busen, M. Saab, Z. Zhang, L. Falivene, G. Pisanò, K. V. Hecke, L. Cavallo, C. S. J. Cazin, A. Steffen and S. P. Nolan, *Chem. – Eur. J.*, 2021, **27**, 11904–11911 [CrossRef](#) [CAS](#) [PubMed](#) ; (d) S. Witzel, A. S. K. Hashmi and J. Xie, *Chem. Rev.*, 2021, **121**, 8868–8925 [CrossRef](#) [CAS](#) .
6. (a) P. Rajakannu, H. S. Kim, W. Lee, A. Kumar, M. H. Lee and S. Yoo, *Inorg. Chem.*, 2020, **59**, 12461–12470 [CrossRef](#) [CAS](#) ; (b) A. B. Maurer and G. J. Meyer, *J. Am. Chem. Soc.*, 2020, **142**, 6847–6851 [CrossRef](#) [CAS](#) [PubMed](#) .
7. M. J. Leitl, D. M. Zink, A. Schinabeck, T. Baumann, D. Volz and H. Yersin, *Top. Curr. Chem.*, 2016, **374**, 25 [CrossRef](#) [PubMed](#) .
8. (a) A. S. Romanov, S. T. E. Jones, Q. Gu, P. J. Conaghan, B. H. Drummond, J. Feng, F. Chotard, L. Buizza, M. Foley, M. Linnolahti, D. Credgington and M. Bochmann, *Chem. Sci.*, 2020, **11**, 435–446 [RSC](#) ; (b) M. Gernert, L. Balles-Wolf, F. Kerner, U. Müller, A. Schmiedel, M. Holzapfel, C. M. Marian, J. Pflaum, C. Lambert and A. Steffen, *J. Am. Chem. Soc.*, 2020, **142**, 8897–8909 [CrossRef](#) [CAS](#) [PubMed](#) .
9. (a) J.-G. Yang, X.-F. Song, G. Cheng, S. Wu, X. Feng, G. Cui, W.-P. To, X. Chang, Y. Chen, C.-M. Che, C. Yang and K. Li, *ACS Appl. Mater. Interfaces*, 2022, **14**, 13539–13549 [CrossRef](#) [CAS](#) [PubMed](#) ; (b) E. A. Martynova, T. Scattolin, E. Cavarzerani, M. Peng, K. V. Hecke, F. Rizzolio and S. P. Nolan, *Dalton Trans.*, 2022, **51**, 3462–3471 [RSC](#) ; (c) I. I. Hashim, N. V. Tzouras, W. Janssens, T. Scattolin, L. Bourda, S. Bhandary, K. V. Hecke, S. P. Nolan and C. S. J. Cazin, *Chem. – Eur. J.*, 2022, **28**, e202201224 [Search PubMed](#) ; (d) N. V. Tzouras, T. Scattolin, A. Gobbo, S. Bhandary, F. Rizzolio, E. Cavarzerani, V. Canzonieri, K. V. Hecke, G. C. Vougioukalakis, C. S. J. Cazin and S. P. Nolan, *ChemMedChem*, 2022, **17**, e202200135 [CrossRef](#) [CAS](#) [PubMed](#) .
10. A. Ruduss, B. Turovska, S. Belyakov, K. A. Stucere, A. Vembris, G. Baryshnikov, H. Ågren, J.-C. Lu, W.-H. Lin, C.-H. Chang and K. Traskovskis, *ACS Appl. Mater. Interfaces*, 2022, **14**, 15478–15493 [CrossRef](#) [CAS](#) .

11. E. A. Martynova, V. A. Voloshkin, S. G. Guillet, F. Bru, M. Beliš, K. V. Hecke, C. S. J. Cazin and S. P. Nolan, *Chem. Sci.*, 2022, **13**, 6852–6857 [RSC](#) .
12. V. G. Andrianov, Y. T. Struchkov and E. R. Rossinskaja, *Chem. Commun.*, 1973, 338–339 [RSC](#) .
13. (a) T. Lauterbach, A. M. Asiri and A. S. K. Hashmi, in *Advances in Organometallic Chemistry*, ed. P. J. Pérez, Academic Press, 2014, vol. 62, pp. 261–297 [Search PubMed](#) ; (b) A. S. K. Hashmi, *Acc. Chem. Res.*, 2014, **47**, 864–876 [CrossRef](#) [CAS](#) [PubMed](#) ; (c) A. Gómez-Suárez and S. P. Nolan, *Angew. Chem., Int. Ed.*, 2012, **51**, 8156–8159 [CrossRef](#) ; (d) F. F. Mulks, P. W. Antoni, J. H. Gross, J. Graf, F. Rominger and A. S. K. Hashmi, *J. Am. Chem. Soc.*, 2019, **141**, 4687–4695 [CrossRef](#) [CAS](#) [PubMed](#) .
14. (a) T. A. C. A. Bayrakdar, F. Nahra, D. Ormerod and S. P. Nolan, *J. Chem. Technol. Biotechnol.*, 2021, **96**, 3371–3377 [CrossRef](#) ; (b) T. A. C. A. Bayrakdar, F. Nahra, J. V. Davis, M. M. Gamage, B. Captain, M. Temprado, M. Marazzi, M. Saab, K. V. Hecke, D. Ormerod, C. D. Hoff and S. P. Nolan, *Organometallics*, 2020, **39**, 2907–2916 [CrossRef](#) ; (c) T. A. C. A. Bayrakdar, T. Scattolin, X. Ma and S. P. Nolan, *Chem. Soc. Rev.*, 2020, **49**, 7044–7100 [RSC](#) .
15. (a) R. W. Y. Man, C.-H. Li, M. W. A. MacLean, O. V. Zenkina, M. T. Zamora, L. N. Saunders, A. Rousina-Webb, M. Nambo and C. M. Crudden, *J. Am. Chem. Soc.*, 2018, **140**, 1576–1579 [CrossRef](#) [CAS](#) [PubMed](#) ; (b) H. Shen, S. Xiang, Z. Xu, C. Liu, X. Li, C. Sun, S. Lin, B. K. Teo and N. Zheng, *Nano Res.*, 2020, **13**, 1908–1911 [CrossRef](#) [CAS](#) ; (c) H. Yi, K. M. Osten, T. I. Levchenko, A. J. Veinot, Y. Aramaki, T. Ooi, M. Nambo and C. M. Crudden, *Chem. Sci.*, 2021, **12**, 10436–10440 [RSC](#) ; (d) M. Jin, R. Ando, M. J. Jellen, M. A. Garcia-Garibay and H. Ito, *J. Am. Chem. Soc.*, 2021, **143**, 1144–1153 [CrossRef](#) [CAS](#) [PubMed](#) .
16. (a) N. Mirzadeh, T. S. Reddy and S. K. Bhargava, *Coord. Chem. Rev.*, 2019, **388**, 343–359 [CrossRef](#) [CAS](#) ; (b) N. Mirzadeh, M. A. Bennett and S. K. Bhargava, *Coord. Chem. Rev.*, 2013, **257**, 2250–2273 [CrossRef](#) [CAS](#) .
17. (a) A. A. D. Tulloch, A. A. Danopoulos, S. Winston, S. Kleinhenz and G. Eastham, *J. Chem. Soc., Dalton Trans.*, 2000, 4499–4506 [RSC](#) ; (b) B. Dutta, R. Schwarz, S. Omar, S. Natour and R. Abu-Reziq, *Eur. J. Org. Chem.*, 2015, 1961–1969 [CrossRef](#) [CAS](#) ; (c) Y. Du, H. Tang, H. Ding, Y. Shi, C. Cao and G. Pang, *J. Chem. Res.*, 2016, **40**, 735–739 [CrossRef](#) [CAS](#) ; (d) E. Tkatchouk, N. P. Mankad, D. Benitez, W. A. Goddard and F. D. Toste, *J. Am. Chem. Soc.*, 2011, **133**, 14293–14300 [CrossRef](#) [CAS](#) [PubMed](#) ; (e) T. A. C. A. Bayrakdar, F. Nahra, J. V. Davis, M. M. Gamage, B. Captain, M. Temprado, M. Marazzi, M. Saab, K. V. Hecke, D. Ormerod, C. D. Hoff and S. P. Nolan, *Organometallics*, 2020, **39**, 2907–2916 [CrossRef](#) ; (f) M. C. Dietl, V. Vethacke, A. Keshavarzi, F. F. Mulks, F. Rominger, M. Rudolph, I. A. I. Mkhaldid and A. S. K. Hashmi, *Organometallics*, 2022, **41**, 802–810 [CrossRef](#) [CAS](#) .
18. (a) F. Strieth-Kalthoff, M. J. James, M. Teders, L. Pitzer and F. Glorius, *Chem. Soc. Rev.*, 2018, **47**, 7190–7202 [RSC](#) ; (b) T. Patra, S. Mukherjee, J. Ma, F. Strieth-Kalthoff and F. Glorius, *Angew. Chem., Int. Ed.*, 2019, **58**, 10514–10520 [CrossRef](#) [CAS](#) [PubMed](#) ; (c) F. Strieth-Kalthoff and F. Glorius, *Chem*, 2020, **6**, 1888–1903 [CrossRef](#) [CAS](#) .
19. (a) S. A. Díaz, D. A. Hastman, I. L. Medintz and E. Oh, *J. Mater. Chem. B*, 2017, **5**, 7907–7926 [RSC](#) ; (b) J. Ling and C. Z. Huang, *Anal. Methods*, 2010, **2**, 1439–1447 [RSC](#) ; (c) L. Zhang, X. Si, F. Rominger and A. S. K. Hashmi, *J. Am. Chem. Soc.*, 2020, **142**, 10485–10493 [CrossRef](#) [CAS](#) [PubMed](#) ; (d) S. Xia and J. Xie, *Gold Bull.*, 2022, **55**, 123–127 [CrossRef](#) [CAS](#) .

20. M. Zhu, C. Zheng, X. Zhang and S.-L. You, *J. Am. Chem. Soc.*, 2019, **141**, 2636–2644 [CrossRef](#) [CAS](#) [PubMed](#) .
21. E. Stempel and T. Gaich, *Acc. Chem. Res.*, 2016, **49**, 2390–2402 [CrossRef](#) [CAS](#) [PubMed](#) .